



**FP7 PROGRAMME**

**DORIS - Ground Deformations Risk Scenarios:  
an Advanced Assessment Service**

GRANT AGREEMENT No. 242212

COLLABORATIVE PROJECT

START DATE: 1 OCTOBER 2010

**WP3 – Value added research and technology  
development**

**DELIVERABLE No. D3.2**

**Exploitation of large archives of existing C-band space-borne SAR  
data**

## DOCUMENT INFORMATION

Organization of lead beneficiary of this deliverable	UNIFI
Work package contributing to the deliverable	WP 3
Contractual Date of Delivery	Month 18
Actual Date of Delivery	April 2012
Nature	O
Dissemination level	PP

<b>Document Responsible</b>	Nicola Casagli (UNIFI)
<b>Authors</b>	Sandro Moretti (UNIFI), Chiara Del Ventisette (UNIFI), Andrea Ciampalini (UNIFI), Davide Colombo (TRE), Oscar Mora (ALTAM), Tazio Strozzi (GAMMA), Fabiana Calò (CNR), Michele Manunta (CNR), Luca Paglia (CNR), Paola Reichenbach (CNR), Inmaculada Garcia (IGME), Rosa Mateos (IGME), Gerardo Herrera (IGME), Balázs Füsi (ELGI)
<b>Version</b>	1.0

## Reference documents

- [DR1] Annex I Description of Work (DoW) of DORIS – “Ground Deformations Risk Scenarios: an Advanced Assessment Service” project - GRANT AGREEMENT NO. 242212.
- [DR2] Deliverable 3.1 – “Reply to the user requirements and establishment of a common framework for RTD activity”.
- [DR3] Deliverable 5.1 – “Large scale thematic maps for selected test-sites (1:50.000)”.

## LIST OF ACRONYMS AND ABBREVIATIONS

ALOS	Advanced Land Observing Satellite
ALTAM	ALTAMIRA Information
ASAR	Advanced SAR
CNR	Consiglio Nazionale delle Ricerche
COSMO-SkyMed	Constellation of Small Satellites for Mediterranean basin Observation
DEM	Digital Elevation Model
DInSAR	Differential SAR Interferometry
DORIS	Ground Deformation Risk Scenarios: an advanced assessment service
DPC	Dipartimento di Protezione Civile
ELGI	Eötvös Loránd Geophysical Institute of Hungary
ENVISAT	Environmental Satellite
EO	Earth Observation
ERS	European Remote-Sensing Satellite
ESA	European Space Agency
EU	European Union
FOEN	Federal Office for the Environment
GAMMA	Gamma Remote Sensing AG
IGME	Instituto Geológico y Minero de España
InSAR	Interferometric Synthetic Aperture Radar
IPTA	Interferometric Point Target Analysis
IREA	Istituto per il Rilevamento Elettromagnetico dell'Ambiente
IUGS-WGL	International Union of Geological Science Working Group on Landslides
LOS	Line Of Sight
MHz	Megahertz
PGI	Polish Geological Institute
POLIMI	Politecnico di Milano
PREVIEW	PREvention, Information and Early Warning pre-operational services to support the management of risks
PS	Permanent/ Persistent Scatterer
PSI	Persistent Scatterers Interferometry
PSInSAR™	Permanent Scatterers Interferometry SAR
RTD	Research and Technological Development
SAR	Synthetic Aperture Radar



---

SBAS	Small BAseline Subset
SPN	Stable Point Network
TRE	Tele-Rilevamento Europa
UNIFI	Università di Firenze
VHR	Very High Resolution
WP	Work Package



---

## EXECUTIVE SUMMARY

In the DORIS project, Work package 3 (Value added research and technology development) is focused on innovative research initiative aimed at improving the exploitation of the existing capabilities of EO data and technology to forecast and manage natural and human induced hazards and risks. WP3 is responsible for the definition of innovative procedures to use EO data and technology for ground deformation assessment in agreement with the Users requirements. WP3 also is focused on the improvement of EO data exploitation for a downstream service.

In this document, the results of the application of new algorithms developed to reconstruct long time series (more than 15 years) of archive data derived from C-band satellite (ERS-1, ERS-2, ENVISAT) are described. These results could be applied to geohazards mapping in the framework of the Emergency Core Service.

## Table of Contents

1.	Introduction.....	6
2.	Description of Developed procedure.....	7
2.1.	SBAS .....	7
2.2.	ERS - ENVISAT Stitching .....	8
2.3.	SPN.....	8
2.4.	IPTA .....	9
3.	RESULTS.....	10
3.1.	Central Umbria (Italy) .....	10
3.1.1.	Considered phenomena .....	10
3.1.2.	Application of the procedure.....	11
3.2.	Messina Province (Italy).....	16
3.2.1.	Considered phenomena .....	16
3.2.2.	Application of the procedure.....	16
3.3.	Dunaszekcső, Rácalmás and Hollóháza (Hungary).....	20
3.3.1.	Considered phenomena .....	20
3.3.2.	Application of the procedure.....	21
3.4.	Silesian Coal Basin (Poland).....	25
3.4.1.	Considered phenomena .....	25
3.4.2.	Application of the procedure.....	25
3.5.	Tramuntana Range (Mallorca) .....	27
3.5.1.	Considered phenomena .....	27
3.5.2.	Application of the procedure.....	27
3.6.	St. Moritz (Switzerland).....	29
3.6.1.	Considered phenomena .....	29
3.6.2.	Application of the procedure.....	29
3.7.	Zermatt (Switzerland).....	34
3.7.1.	Considered phenomena .....	34
3.7.2.	Application of the procedure.....	34
4.	DISCUSSION.....	37
4.1.	Advantages.....	37
4.2.	Disadvantages .....	37

## 1. INTRODUCTION

DORIS intends to go beyond the state-of-the-art in the science and the technology currently used for the detection, mapping, monitoring and forecasting of ground deformations, at different geographical scales and in various physiographic environments.

Significant improvements are expected from the multifaceted application of DInSAR technology. DORIS intends to fully exploit the existing ESA Synthetic Aperture Radar (SAR) archives, operating in the microwave C-band. The availability of a large number of radar satellite images with an interferometric revisit time of 35 days, based on exploiting the ERS and ENVISAT archives, allowed in many cases analyzing the historical evolution of the displacements from 1991 to present. Monitoring of slow moving mass movements can greatly benefit from the differed-time detection of displacements on slow to very slow landslides by means of space-borne differential interferometry. The understanding of the long-term behaviour of such phenomena, which display episodic partial or total reactivations, plays a key role for planning emergency responses over periods of critical meteo-hydro-geological conditions.

The temporal continuity and the geometric compatibility among time series of ERS-1, ERS-2 and ENVISAT data represent an unprecedented opportunity to generate very long time series of ground deformations. This will provide exclusive information for an improved understanding of the long term behavior of slow and very-slow ground deformation phenomena. Furthermore, DORIS intends to extensively exploit the catalogues of multiple C-band SAR sensors (e.g., ERS-ENVISAT) to provide, via a joint analysis, additional information on ground displacements.

This document provides a detailed description on the possibility of generating very long deformation time series (almost 20 years) by properly merging the ERS-1/2 and ENVISAT datasets. This procedure could represent the baseline for the Emergency Core Service for Landslides, whose information serves as a framework for a better planning and implementation of Downstream Services. The technological research gaps and the general problems related to the combined use of different radar sensors are addressed in this document.

## 2. DESCRIPTION OF DEVELOPED PROCEDURE

### 2.1. SBAS

The key point at the base of the Small BAseline Subset (SBAS) technique (Berardino et al. 2002) is the selection of the SAR data pairs used for generating the interferograms. Indeed, the SBAS approach relies on the use of a large number of SAR acquisitions and implements an easy combination of small spatial and temporal separation (baseline) interferograms computed from these data in order to mitigate the noise effects (referred to as decorrelation phenomena) thus maximizing the number of reliable measure pixels.

Originally designed for investigating deformation phenomena extending over very large areas, the SBAS algorithm has been subsequently extended in order to analyse also localized phenomena affecting human-made features and individual slopes. As result, the SBAS analysis can be currently carried out at two spatial scales, namely at regional and local scale (Lanari et al. 2004). At the regional scale, the technique exploits average (multi-look) interferograms to produce deformation maps of wide areas (100 km x 100 km in the ERS and ENVISAT case) at low spatial resolution scale (about 100 m x 100 m in the ERS and ENVISAT case); at the local scale, single-look interferograms are exploited in order to generate deformation maps at the full spatial resolution scale (about 5 m x 20 m in the ERS and ENVISAT case), thus allowing to focus on local deformation affecting single elements at risk. At both scales, time-series showing the temporal evolution of surface displacements are generated.

In the framework of the DORIS project, the SBAS technique has been further extended in order to apply such multi-scale analysis to multi-sensor SAR data collected by different radar systems acquiring with the same illumination geometry as for the case of ERS-1/2 and ENVISAT satellites (Bonano et al. 2012). This development allows to effectively exploit the large available SAR data archive for the analysis of slow-moving deformation phenomena, such as landslides and subsidences, through the generation of very long term deformation time-series spanning almost 20 years.

The basic issue of the multi-sensor SBAS approach is to consider the images acquired by the ERS and ENVISAT sensors as belonging to independent subsets (Pepe et al. 2005); accordingly, no ERS/ENVISAT cross-interferograms, characterized by heavy decorrelation effects due to slightly different carrier frequencies of the two radar systems, are generated and the integration of ERS/ERS and ENVISAT/ENVISAT interferograms is effectively performed by applying the conventional SBAS strategy without major changes. Moreover, the multi-sensor SBAS approach effectively exploits the Doppler centroid variations of the post-2000 ERS-2 acquisitions and the carrier frequency difference between the ERS-1/2 and the ENVISAT systems for maximizing the number of investigated SAR pixels, identifying also those exhibiting a response significantly deviating from a single scatterer backscattering, and improving their geocoding as well



## 2.2. ERS - ENVISAT Stitching

After the failure of ERS-2 gyroscope, the updating of ERS PS measurements by means of the Advanced SAR (ASAR) data became a major issue. Apart from the enhanced ASAR features in terms of acquisition modes and polarimetric capabilities, the main difference between ERS and ENVISAT ERS-like acquisitions is the carrier frequency (5.3GHz for ERS-1/2 and 5.331GHz for ENVISAT). The 31MHz frequency shift has a major impact on any interferometric application involving ERS-ENVISAT data-sets since the bandwidth of both systems is less than 18MHz. ERS-ENVISAT interferograms usually turn out to be completely decorrelated, at least for typical baseline values (< 1300m), since no common band is available for distributed targets. Point targets, on the contrary, are expected to remain coherent and their ERS-ENVISAT phase histories can be coherently stitched.

Considering the interferometric phase between a ERS and a ENVISAT acquisition, it can be demonstrated that together with the common phase terms related to motion, topography and atmosphere, there is an additional contribution which varies from point to point but it is constant in all the ERS-ENVISAT interferograms:

$$\Delta\varphi = \frac{4\pi}{c} \Delta f \Delta r$$

where  $c$  is the speed of light,  $\Delta f$  is the difference between the ERS and ENVISAT carrier frequency and  $\Delta r$  is the slant range subpixel position of the scatterer.

This term is referred to as the Location Phase Screen (LPS). Given the 31MHz frequency shift, the LPS changes by almost two cycles across a single slant-range resolution cell, so it is extremely sensitive to the target slant-range position within the resolution cell.

Estimating this contribution for each scatterer together with the velocity and DEM error contribution, allows to remove it from the ERS-ENVISAT interferograms, making possible the generation of time series of displacements spanning the whole time period covered by the 2 datasets.

## 2.3. SPN

ALTAMIRA INFORMATION has processed C-band SAR data using its SPN (Stable Point Network) technique. This software uses a stack of SAR images to measure ground deformations with millimetric precision. During the processing, the ground scatterers not affected by temporal decorrelation are identified; these are called persistent scatterers or stable points. They are natural objects over the ground surface that give a very good reflection to the satellite throughout the entire stack of images. These points present a reduced level of noise, which allows for very reliable measurements. Furthermore, the atmospheric effects are estimated and compensated during the processing to derive highly accurate elevation and displacement values for each stable point. The highly precise error compensation allows for the generation of

time series charts that provide a visualisation of the evolution of the displacement of each stable point. Urban, semi-urban or rural areas can be studied in great detail, both in terms of high spatial resolution and the historical variation of the displacement over long time periods.

Separate processing have been performed for ERS-1/2 and ENVISAT data, in order to generate a complete history of the terrain deformation, but using the same methodology. This allows generating independent maps for different temporal periods with a higher density of measured points, since temporal decorrelation is lower for shorter temporal periods.

## 2.4. IPTA

Interferometric Point Target Analysis (IPTA) is a method to exploit the temporal and spatial characteristics of interferometric signatures collected from point targets to accurately map surface deformation histories, terrain heights, and relative atmospheric path delays. The use of targets with point like scatter characteristics has the advantage that there is much less geometric decorrelation. This permits phase interpretation even for large baselines above the critical. Consequently, more image pairs may be included in the analysis and this improves the temporal sampling. Another important advantage is the potential to find scatterers in low-coherence areas. Finding usable points in low-coherence regions fills spatial gaps in the deformation maps. For a more detailed discussion of the point target based interferometric technique used see (Wegmüller et al., 2004).

There is a high interest in the possibility to continue deformation monitoring between the rich archive of SAR data acquired by the ERS and ENVISAT satellites. ENVISAT operated in the same tracks as the ERS satellites, nevertheless at a slightly different carrier frequency, which has a strong influence on across-sensor interferometry (Wegmüller et al., 2005). In addition, the differences in the range and azimuth pixel spacing must be considered in the co-registration of ERS and ENVISAT Single-Look Complex (SLC) data.

Our approach for the integration of ERS and ENVISAT data into IPTA processing takes advantage of the use of targets with point like scatter characteristics because coherence is maintained for many scatterers across series including both ERS and ENVISAT data – this in spite of the slightly different sensor carrier frequencies. Nevertheless, because for many other targets the coherence across the stacks of ERS and ENVISAT data is not guaranteed, across-sensor (i.e. between ERS and ENVISAT) interferograms are not considered. Instead, separate IPTA processing (i.e. with one central reference for ERS and one central reference for ENVISAT) are performed on images co-registered to the same geometric reference (either ERS and ENVISAT) and for a list of candidate point targets resulting from merging the lists computed separately with ERS and ENVISAT data. With this approach, results on the same targets can be easily compared while maintaining the maximum number of valid points for both ERS and ENVISAT data. Another implication of our approach is that two temporal

references, one for ERS and one for ENVISAT, exist and there is therefore not a single time series.

### 3. RESULTS

In this section the considered phenomena which characterize each test site will be briefly described. Moreover the results obtained using the methodologies developed by the data providers are reported.

#### 3.1. Central Umbria (Italy)

##### 3.1.1. Considered phenomena

The Ivancich landslide area is located in Assisi, Italy. The town of Assisi extends along the NE sector of the mountain ridge represented by the Monte Subasio, a distinct physiographical feature in central Umbria, and is bounded to the SW by the ample Valle Umbra plain (figure 1A). Sedimentary rocks crop out in the area. Layered and massive limestone, marl, and clay pertaining to the Umbria-Marche stratigraphic sequence, Lias to Eocene in age, are overlaid by lake deposits, lower Pliocene to Quaternary in age, and by fluvial deposits, recent in age.

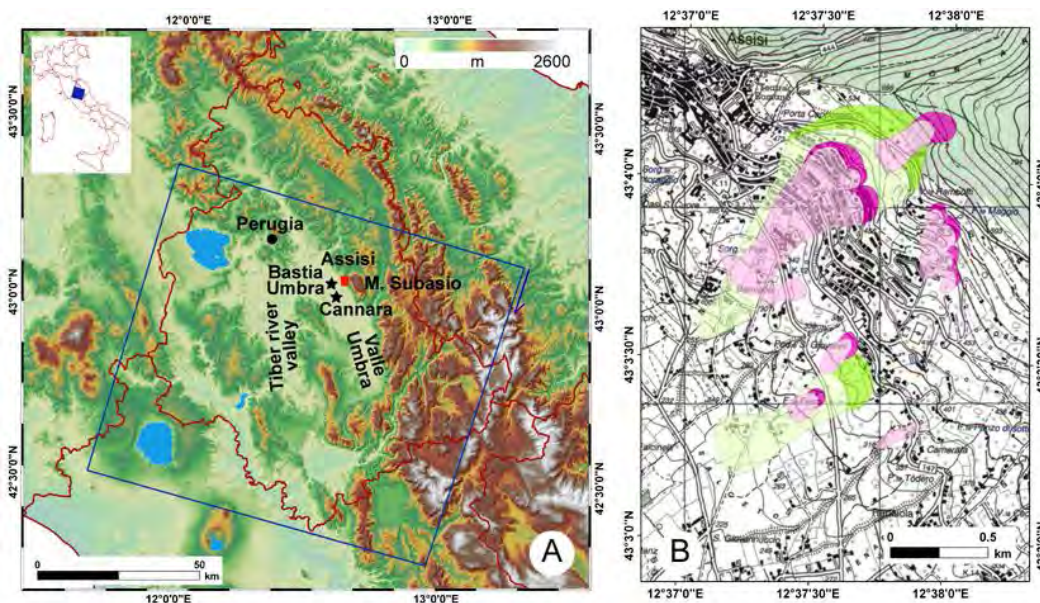


Figure 1. (A) Map showing terrain in Umbria, Italy. The study area, shown by the red polygon, is located in Assisi. The blue line shows the area covered by the ERS-1/2 and the ENVISAT radar images used in this study. Stars indicate the location of two rain gauges used in the analysis. (B) Map showing landslides in the Ivancich landslide area, and the neighboring territory in Assisi. Green polygons are old landslides and purple polygons are recent landslides. Landslide crown areas (darker colors) are shown separately from landslide deposits (lighter colors).

Ivancich is a neighborhood in Assisi located SE of the mediaeval part of the town. Built mainly in the period 1960 – 1970, the neighbourhood is a residential area of one- to three-story private homes, along with the Assisi hospital and a Franciscan convent. In the area, a deep-seated landslide is present (figure 1B). Geomorphological, geotechnical, and topographical investigations revealed that the Ivancich landslide is an old (ancient) translational slide that involves the debris deposit that covers the bedrock, represented by a pelitic sandstone unit. More recent, slides have developed inside the old landslide deposit (figure 1B). The recent slope failures have caused damage to roads, private and public buildings, including the Assisi hospital, and retaining structures, since the 1970s.

### 3.1.2. *Application of the procedure*

The multi-scale and multi-sensor SBAS analysis has been carried out by processing both descending and ascending SAR datasets relevant to the Umbria region, (Italy). In particular, the descending dataset is composed of 116 (77 ERS-1/2 and 39 ENVISAT) images and covers the April 1992-September 2010 time interval, while the ascending dataset includes 87 (36 ERS-1/2 and 51 ENVISAT) images spanning from June 1995-September 2010.

As results of the regional scale SBAS analysis, low resolution deformation velocity maps and associated time series from both datasets have been produced, allowing the detection of several natural and human induced phenomena occurring in the study area. Figure 2 reports the low resolution deformation velocity map obtained by processing the descending dataset, superimposed on an amplitude SAR image of the analysed area. Such deformation velocity map reveals an overall stability of the area in the observed time interval. However, significant deformation patterns are present in the Valle Umbra, where a subsidence induced by water exploitation occurs, and in the area around Perugia. We point out that the portion of Valle Umbra between Assisi and Foligno has been affected by subsidence since 1992 (Figure 2c), as already shown by Guzzetti et al. (2009), while the Perugia area exhibits ground deformation only since 2000. This is clearly visible in the plot reported in Figure 2b, thus demonstrating the effectiveness of the multi-scale SBAS approach to analyse and monitor large time intervals (almost 20 years) deformation phenomena, characterized by a temporal evolution of displacements that significantly deviate from a linear trend.

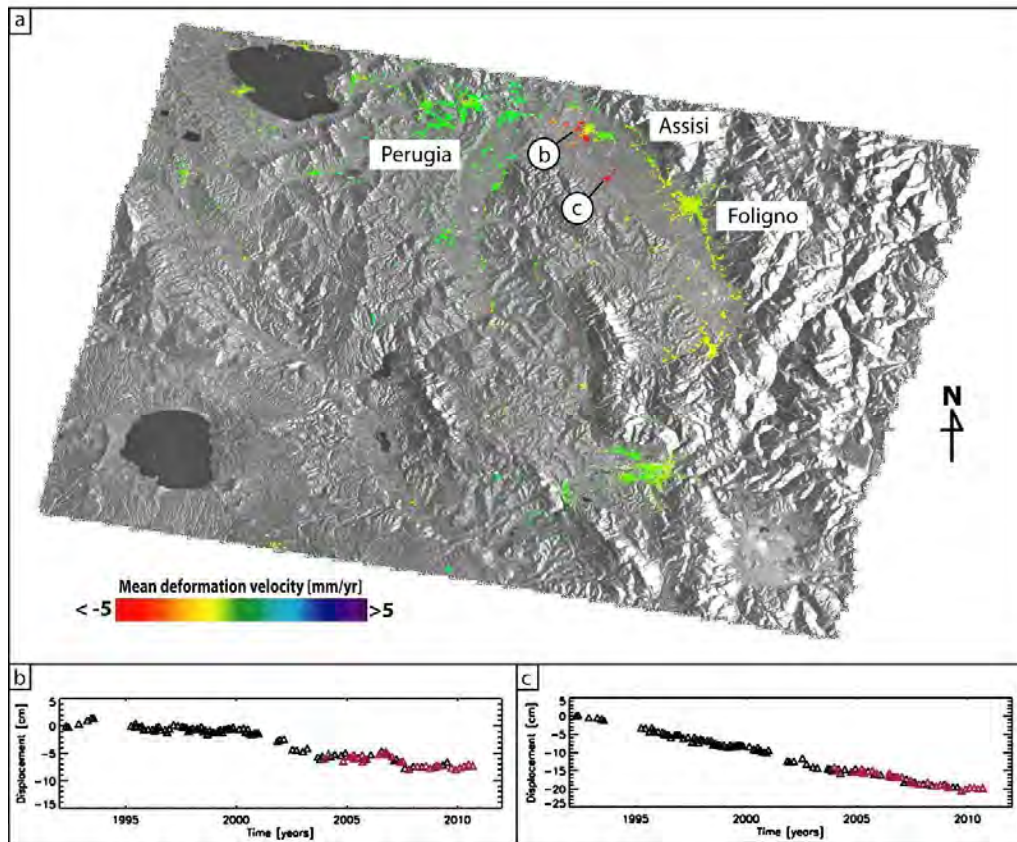


Figure 2. (a) Geocoded mean deformation velocity map at low spatial resolution scale (pixel size  $\approx 100\text{ m} \times 100\text{ m}$ ) of the whole study area, obtained from descending SAR data, and superimposed on the amplitude SAR image. Deformation values are measured along the satellite Line of Sight (LOS). (b) Deformation time series relevant to the pixel labelled as (b) in figure 2(a) is shown. Black and red triangles represent ERS and ENVISAT acquisitions, respectively. (c) Same as (b) but referred to the pixel labelled as (c) in figure 2(a).

Furthermore, the availability of both ascending and descending datasets allows investigating the direction of the retrieved ground movement, by computing its East-West (E-W) and vertical components (the North-South component cannot be singled out because the satellite orbit is nearly polar). In particular, by exploiting the satellite look-angle  $\vartheta$  (assumed to be the same for both orbits) we compute the e-w ( $d_{e-w}$ ) and vertical ( $d_{vert}$ ) components of the detected deformation as follows:

$$d_{vert} = (d_{desc} + d_{asc}) / 2 \cos \vartheta$$

$$d_{e-w} = (d_{desc} - d_{asc}) / 2 \sin \vartheta$$

Where  $d_{desc}$  and  $d_{asc}$  represent the LOS-projected deformation signals computed from descending and ascending datasets, respectively.

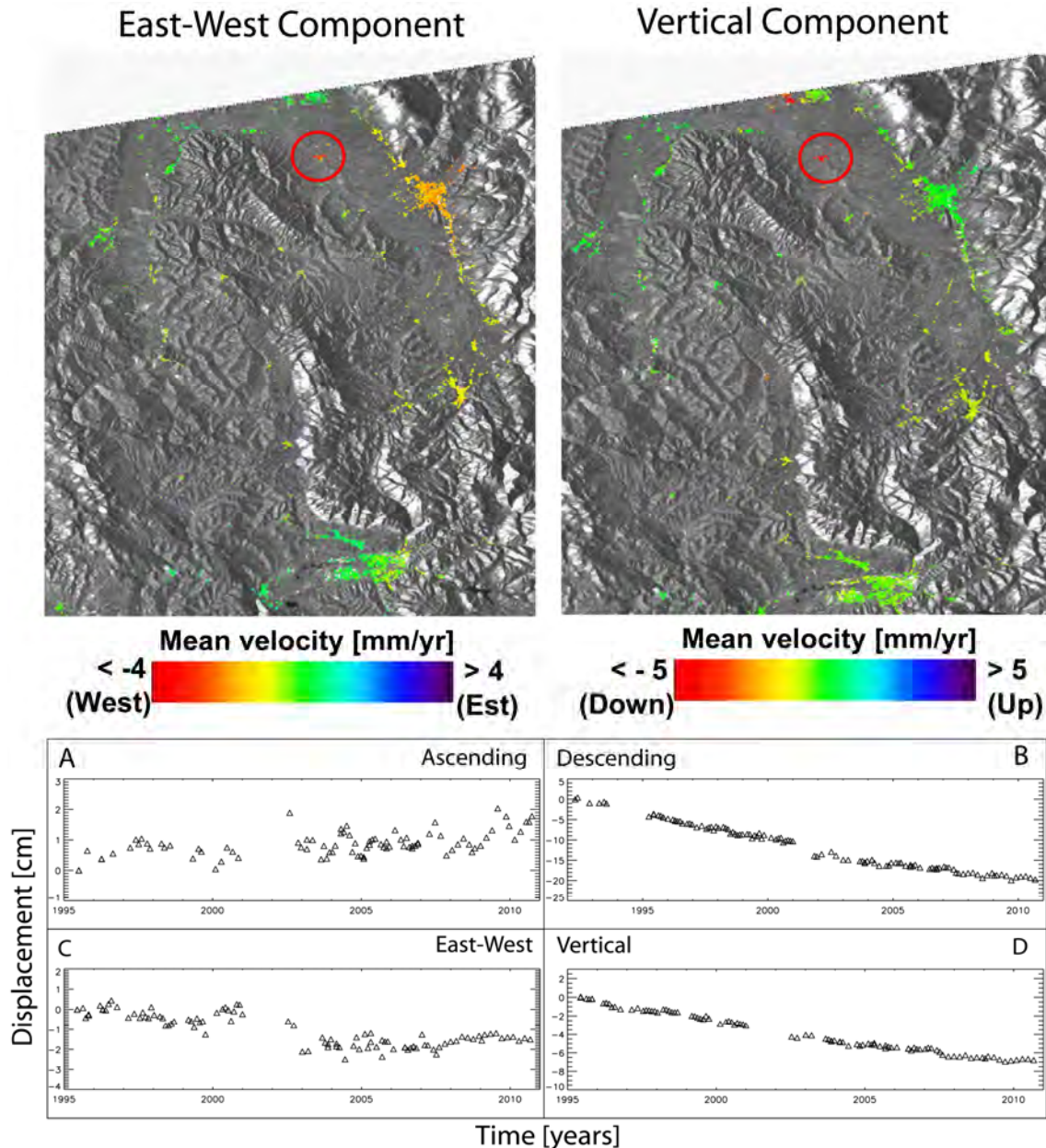


Figure 3. Mean deformation velocity maps relevant to the horizontal (E-W) and vertical displacement components (top), obtained by combining descending and ascending SAR data, and superimposed on the amplitude SAR image. Deformation time-series (bottom) relevant to a measure point (see red circle), located in the Cannara area, affected by subsidence induced by aquifer exploitation. A) displacements along the ascending LOS direction (1995-2010); B) displacements along the descending LOS direction (1992-2010); C) East-West component of the displacements; D) vertical component of the displacements. Note that graphs C and D are related to the common time interval (1995-2010) between ascending and descending datasets.

Figure 3 shows the deformation velocity maps relevant to the vertical and E-W components. A significant example of DInSAR time-series relevant to deformation patterns caused by aquifer exploitation in the Valle Umbra, around the town of Cannara, highlighted by the red circles in Figure 3, is reported. To further investigate the deformation field of this site, we show the ERS-ENVISAT time-series relevant to the ascending and descending LOS-projected displacements, and to the E-W and vertical components (Fig. 3A-D).

The presented case study highlights the effectiveness of the regional scale SBAS approach to detect and investigate the complex behavior of different geological phenomena, allowing us to identify both horizontal and vertical deformation components, also in the case of non-linear displacements.

In order to give more insights on the behavior of localized phenomena, we perform the full resolution multi-sensor SBAS-DInSAR analysis. In particular, we focus here on Assisi where an active slow-moving deep seated landslide affects the Ivancich neighborhood located in the S-E part of the mediaeval town (Fig. 4). Geomorphological analyses and topographical surveys have been performed pointing out that the Ivancich landslide is an old translational slide involving the debris deposit overlaying the bedrock constituted by a pelitic sandstone unit. Recent slides have been developed inside the old landslide body, causing since 1970s severe damage to roads and buildings (see Section 3.1.1). In Figure 4 the full resolution deformation velocity map and the time-series associated to two unstable points located on the landslide body are shown. The SBAS analysis at local scale allowed detecting an active sector clearly showing a deformation trend during the analyzed period (Fig. 4). The results, in good agreement with the damage assessment, reveal that, probably due to differential movements, most of the damage is located along the eastern boundary between the detected active sector and the portion of the slope that is not affected by deformation during the investigated time interval.

The presented results show the effectiveness of the multi-scale and multi-sensor SBAS-DInSAR approach for the detection of ground deformation and for their long-term monitoring at both regional and local scales, thus allowing performing detailed analyses on both the spatial and temporal patterns of such phenomena.

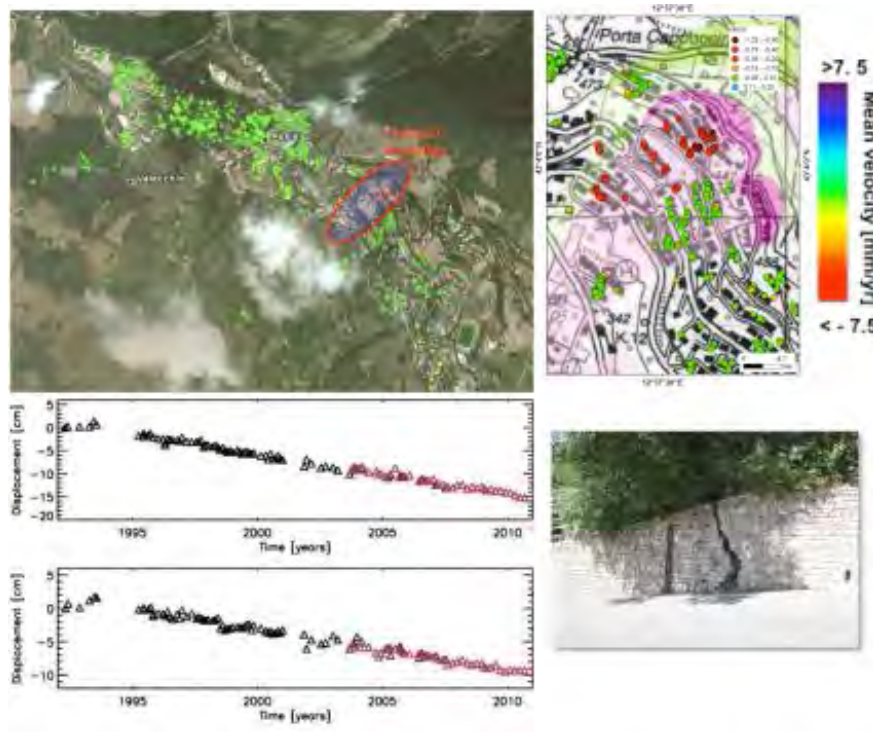


Figure 4. Full resolution deformation velocity map relevant to the Assisi area (upper left) and zoom on the Ivancich landslide (upper right). Deformation time series (lower left) related to two points located within the active zone of the landslide. Damages occurred in the investigated area (lower right).



## 3.2. Messina Province (Italy)

### 3.2.1. *Considered phenomena*

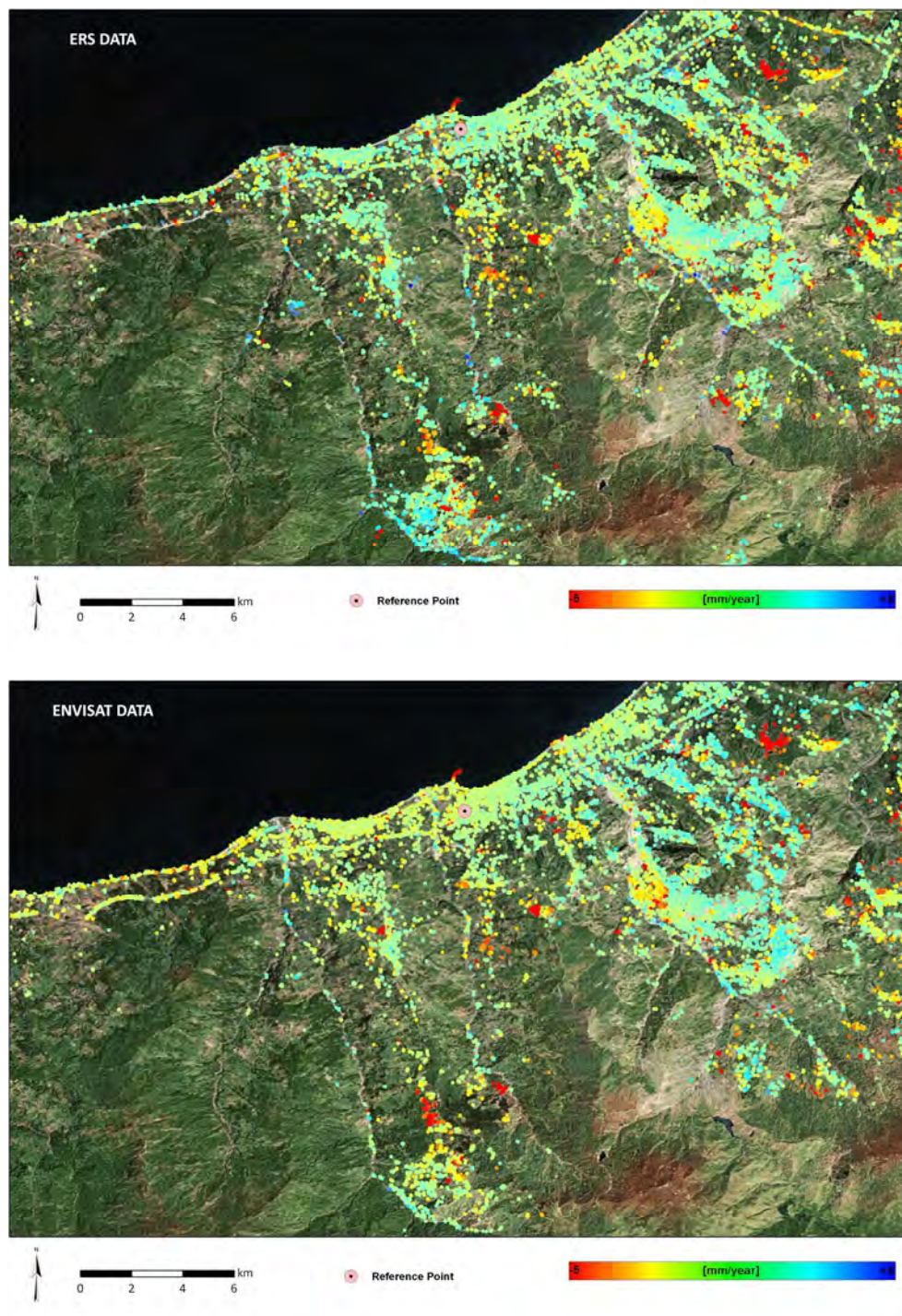
The study area (Monti Nebrodi and Giampilieri) is located along the north eastern part of Sicily (Southern Italy). In the period from October 2009 to February 2010, the area was highly affected by several landslide events that caused intense damages and casualties. The landslide events continue till today as testified by the event occurred during March 2011 in San Fratello where 12 people were evacuated. The Monti Nebrodi ridge is 70 km long with ENE-WSW direction and is part of the Sicilian Apennines. The altitude of the area spans from the sea level to 1847 m (Monte Soro). Intense and exceptional rainfall event was the main factor that, combined with the steep slopes, triggered several slope movements along the Monti Nebrodi. In particular debris flow, rotational and translational slides, rock falls and shallow and deep-seated landslides occur. Giampilieri is located on the eastern coast of Sicily, in the Peloritani Mountain Belt which represents a segment of the Apennine-Maghrebide Orogen. The geomorphology of the area is strongly influenced by the geo-structural conditions, by the crystalline competence of the outcropping rock (mainly medium grade metamorphic rocks) and by the recent tectonic activity. The coastal landscape is typical of the recently uplifted areas: steep slopes, narrow valleys and high relief energy are the main geomorphologic feature. The morphometric characteristics of the river basins, represented by a watercourse network having regular and parallel paths, are influenced by the short distance separating the watershed from the coast. River catchments have a reduced widening with a significant transport of solid materials; incisions are short and deeply entrenched into V-shaped valleys, especially in the mountainous sector. Several small alluvial plains, formed where riverbeds become over-flooded, characterise the coastal area. The presence of the so-called "fiumare", straight, steep course, gravel-bed river draining mountain areas is typical of Mediterranean climate region. Their flow varies seasonally and their regime is torrential with catastrophic transport of solid materials following heavy rainfall, causing severe damage if flooding occurs close to populated centres. In this area the main type of landslides that have occurred can be classified as debris flow and debris avalanches. More than 600 landslides in a day were triggered by exceptionally intense and localized rainfalls.

### 3.2.2. *Application of the procedure*

ERS-ENVISAT Stitching (Merging) analysis of the area (275 km<sup>2</sup>) led to the identification of 26842 total measurement points (MP), with a point density of ~97 PS/km<sup>2</sup>. Figure 5 shows the distribution of the MPs identified compared with single ERS and ENVISAT results.

The distribution of MP within the study area is homogeneous with ERS and ENVISAT results. As far as velocity field is concerned the 'merging velocity'

corresponds generally to the average of ERS and Envisat separate velocity fields. Examples of time series are reported in Figure 6.



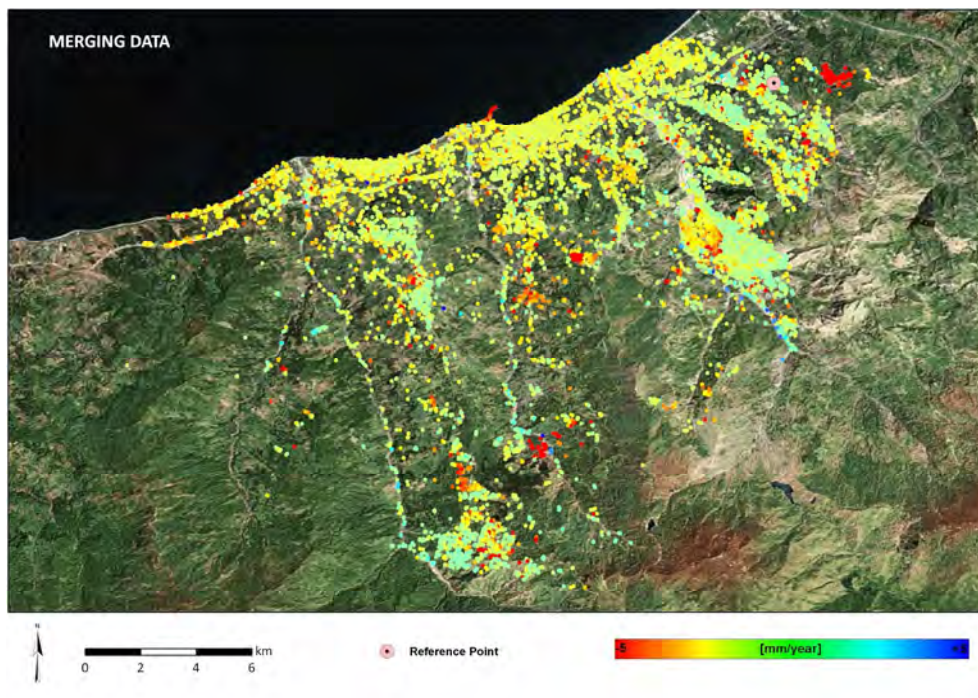


Figure 5. San Fratello Area - SqueeSAR™ results: ERS and ENVISAT data (up) versus Merging data (down).

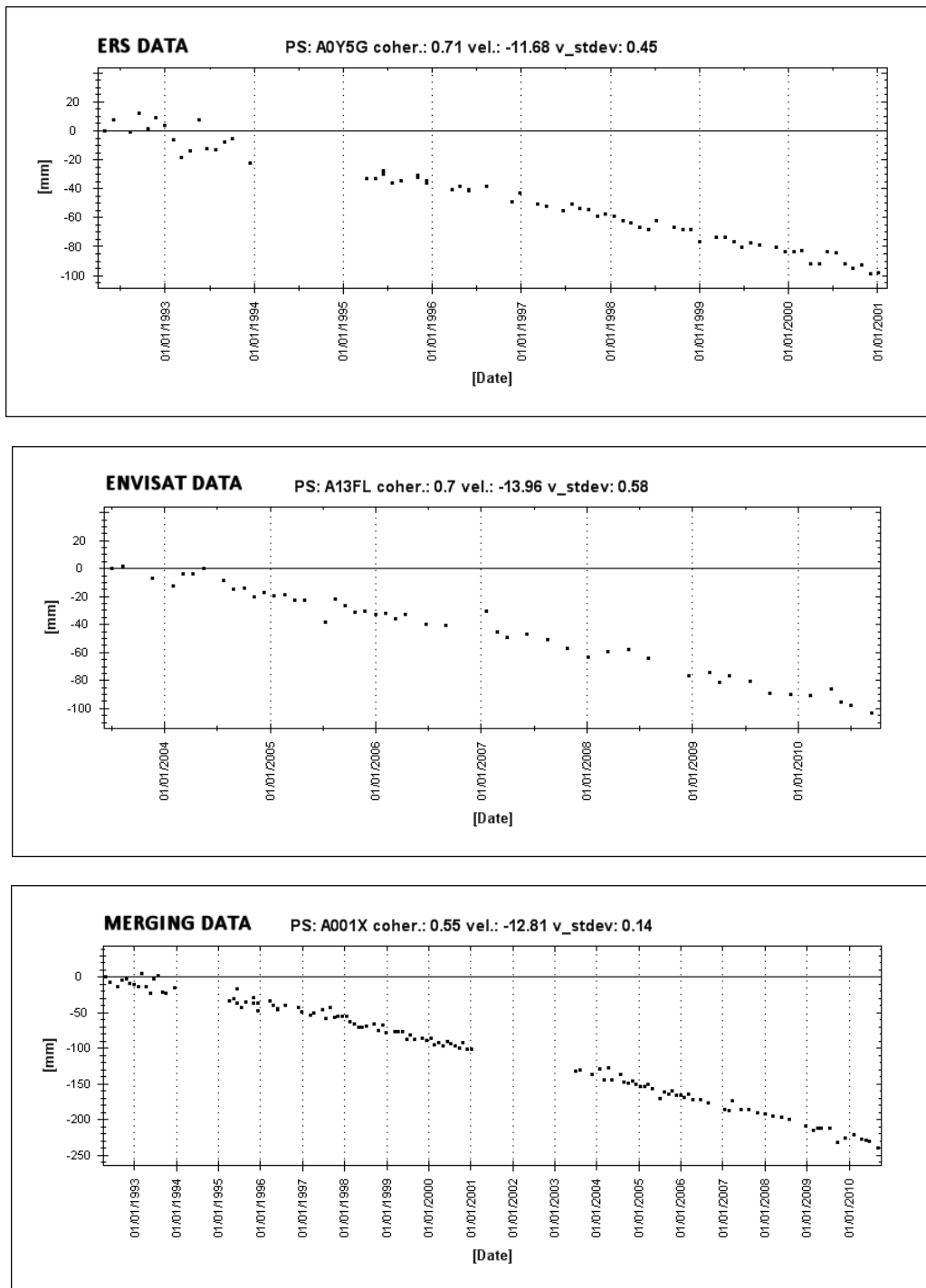


Figure 6. Time series examples.

### 3.3. Dunaszekcső, Rácalmás and Hollóháza (Hungary)

#### 3.3.1. *Considered phenomena*

The Hungarian lowland is located to the south and to the west of the Carpathian mountain range and bounded to the south-east by the Transylvanian Alps. Landscape is characterized by plains, rolling hills and low mountains. The area is drained by tributaries of the Tisza River, which drains into the Danube. Climate is continental to sub-continental, with a mean annual precipitation less than 1000 mm. In the area sedimentary rocks (sandstone and conglomerates), crystalline schist with limestone, and volcanic material crop out. A Loess cover is present in the area. Due to local morphological and geological settings, mass movements of different types are common, and cause extensive damage to buildings and the infrastructure. Three landslide sites have been preliminarily singled out:

(i) The test area covers large part of The Zemplén Mountains. Landslides are very frequent phenomena on the steep valleys of this volcanic mountain. There are more than twenty landslide events registered here, covering almost all types of ground deformations in Hungary. Hollóháza village is situated in a NNW-SSE direction valley in the northern part of Zemplén Mountains. It is 2,5 km along the valley, but only a few hundred meters wide. The foot of the valley in the village is 280-360 m, the surrounding peaks are 450-520 m high. Different thickness rhyolite tuff and sea sediments lie on the base mountain floor. These sediments dip in the direction of the valley forming a natural pervious layer. Another important factor is most bentonitic rhyolite tuff, as well as clay, have high (40-50%) montmorillonite content. The recurring, swelling tuff and clay layers recline on steep volcanic rock and receive their water content through the contact surface. According to the morphological and geological situation the settlement and its close environment have high landslide hazard.

(ii) The Danube river bank of Dunaszekcső is built up of 40 m thick loess dissected by clay stripes, and below this is upper-pannonian sand. The borderline is indefinite, but is around flood level. It is soaked by high groundwater levels, as well as the waters under pressure of the upper-pannonian sand layer tiered up by movements. Consequently, the stability of the steep slopes and rock walls gradually decrease causing surface deformations.

(iii) The Rácalmás area, similar to Dunaszekcső, is on the left bank of the Danube river and is part of the steep, high bank ridge, which can be followed down to the country border. The erosion and collapse of loess's along the Danube, as well as the eastern shores of Lake Balaton and other hilly areas is a general problem in Hungary.

In Rácalmás, on the surface a thick (50 m) of Pleistocene loess bed lays on the upper-pannonian sand and clay layers. In rainy periods or in times of high water level in the Danube these layers get saturated, which causes the development of slides. The morphology of the high banks is also an additional factor.

### 3.3.2. *Application of the procedure*

Altamira has done the PSInSAR processing of the C-band satellite images for the Hungarian test sites in the framework of international cooperation of DORIS.

With the different sensors, 17 years of data have been embraced. The intervals of the observations are not even complete, a lack of data occurs between 2001 and 2003 because of technical problems of the satellites. In the periods when the observations were continuous the time between each measurement was 35 days for ERS and ENVISAT (Tab. 1). The spatial distribution of the scatterers (PS) was good in most cases (4.6 - 87.1 PS/km<sup>2</sup>), especially if we consider that the measurements have been performed on the most problematic areas regarding the method (rarely built-up areas, steep and variable surface, vegetation cover).

Test area	Size of test area (km <sup>2</sup> )	Satellite / Band	Track dir.	Coh. min.	Number of PS	Average density of PS (PS/km <sup>2</sup> )	Start date	End date	No of images	Average observation interval (day)
Rácalmás	513	ERS / C	desc.	0,35	24634	48,0	1992.11.24	2000.12.01	56	53
		ENVISAT / C	desc.	0,35	26853	52,3	2002.11.01	2010.09.10	35	84
Dunaszekcső	153	ERS / C	desc.	0,29	2015	13,2	1992.11.24	2000.12.01	54	56
		ENVISAT / C	desc.	0,37	1917	12,6	2002.11.01	2010.09.10	35	84
Hollóháza	941	ERS / C	desc.	0,33	9454	10,0	1992.05.11	2000.11.09	60	53
		ENVISAT / C	desc.	0,5	4308	4,6	2002.11.14	2007.02.01	22	107

Table 1. The main data of PSInSAR processing

### 3.3.2.1. Dunaszekcso

Figure 7 shows a long time series obtained by joining deformation data from ERS-1/2 and ENVISAT results. The final time series covers the timeframe from 1992 to 2010.

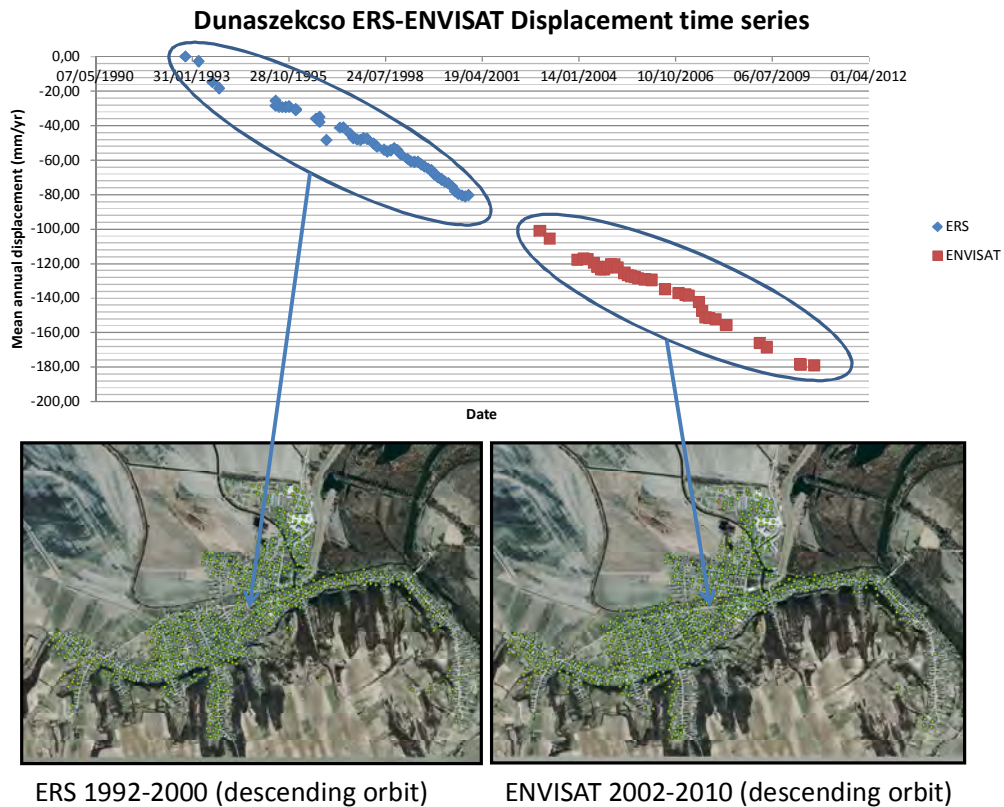


Figure 7. ERS-ENVISAT (descending orbit) displacement time series.

### 3.3.2.2. Hollohaza

The Figure 8 shows a long time series obtained by joining deformation data from ERS-1/2 and ENVISAT results. The final time series covers the timeframe from 1992 to 2009.

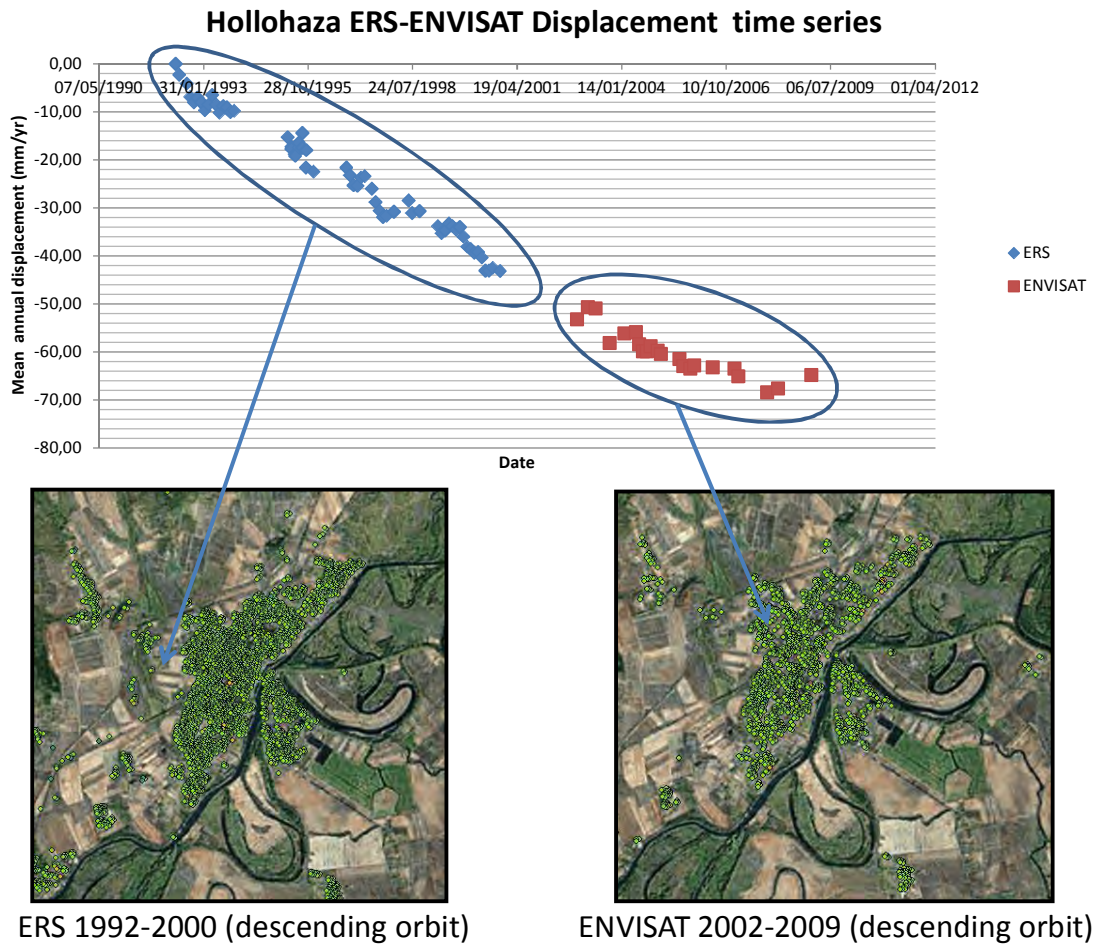


Figure 8. ERS-ENVISAT (descending orbit) displacement time series.



### 3.3.2.3. Racalmas

The following Figure shows a long time series obtained by joining deformation data from ERS-1/2 and ENVISAT results. The final time series covers the timeframe from 1992 to 2010.

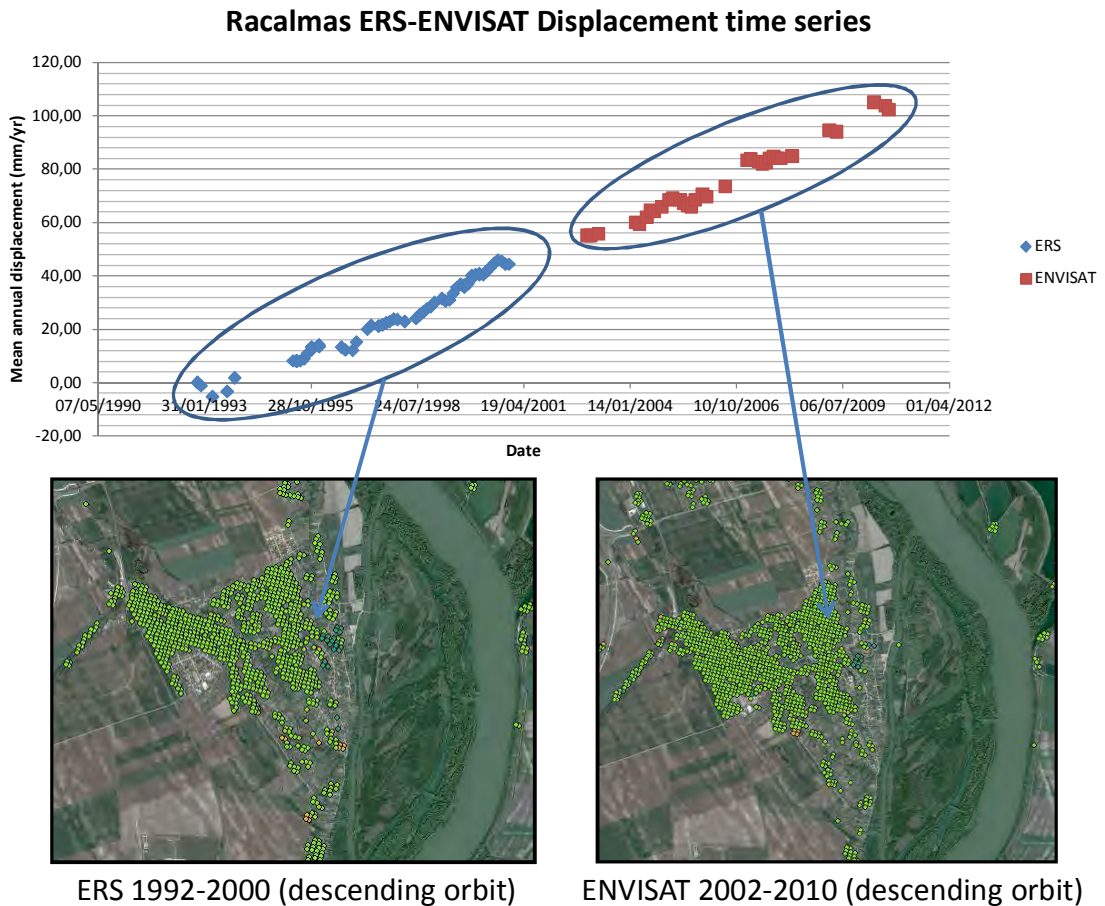


Figure 9. ERS-ENVISAT (descending orbit) displacement time series.

### 3.4. Silesian Coal Basin (Poland)

#### 3.4.1. *Considered phenomena*

The study area is located to the north of the Carpathian mountain range, in the central part of the Upper Silesian Coal Basin (USCB), in southern Poland. Coal mining activity in the USCB has been conducted since the 17th century. In 1979 the largest amount of coal 200x10 Mg/year was mined. At present there are 30 active coal mines in the USCB. Total exploitation of coal is estimated at 70x10<sup>6</sup> Mg/year. In the study area, hazardous ground deformations are caused primarily by the extensive and longwall mining operations, chiefly in the vicinities of the cities of Katowice, Zabrze and Ruda Slaska. The subsidence in Upper Silesia commonly reaches velocities of a few centimeters per month but there are many areas with subsidence of one centimeter daily. Exploitation of coal deposits, conducted in the USCB for over 200 years, has created a complicated state of stress and deformation, which is the cause of dynamic phenomena manifested in the form of rock mass shock. Systematic seismic observations have been here for about 60 years. Currently, Central Mining Institute conducts and develops catalogues "of strong mining tremors" on the basis of data sent by the Upper Silesian Regional seismic network (GRSS) and mining seismological network (KSS).

#### 3.4.2. *Application of the procedure*

Due to the strong non linear displacement occurred in the temporal gap between ERS and ENVISAT, the ERS-ENVISAT Stitching (Merging) analysis has not been performed for the Silesian coal Basin area data. Below, the ERS and ENVISAT deformation velocity maps are reported (Figs. 10 and 11).

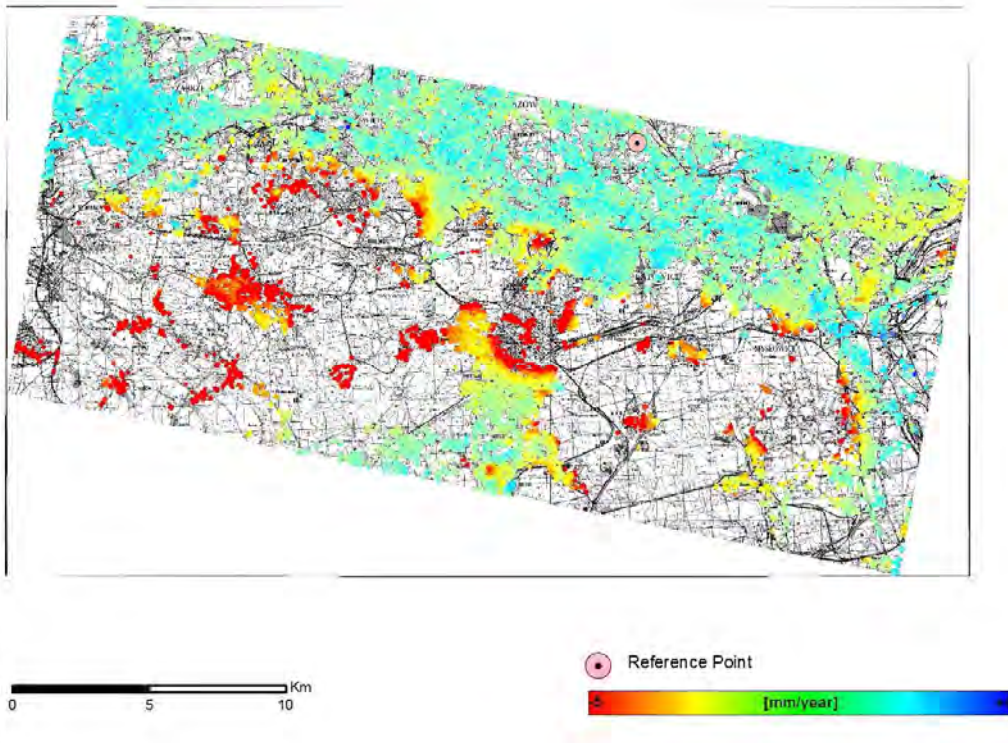


Figure 10. Deformation velocity map obtained by ENVISAT data.

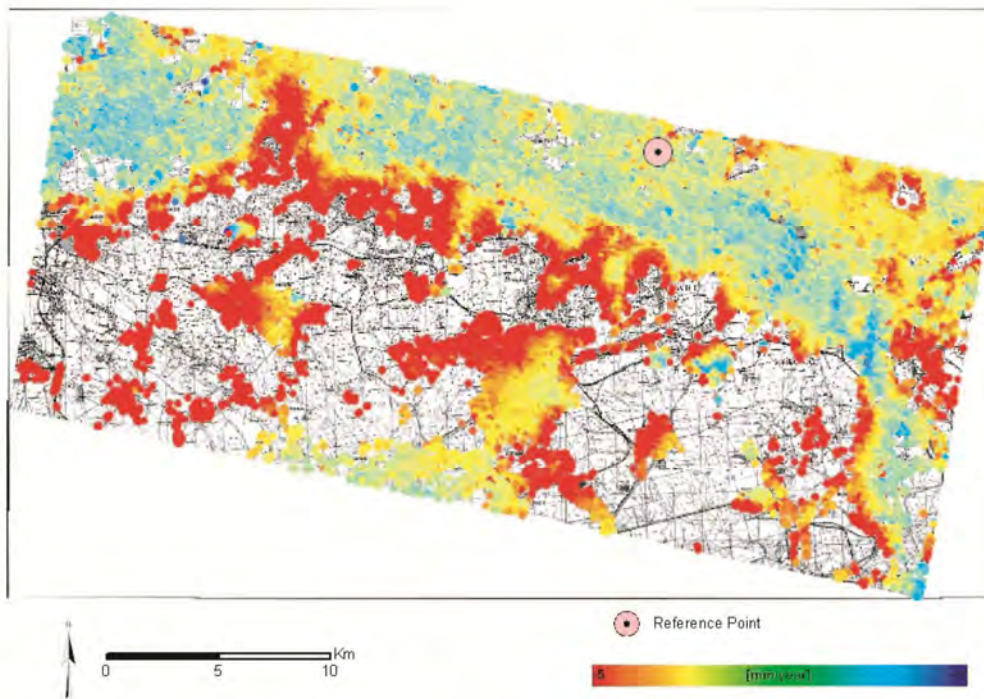


Figure 11. Deformation velocity map obtained by ERS data.

### 3.5. Tramuntana Range (Mallorca)

#### 3.5.1. *Considered phenomena*

The island of Majorca has a variety of different geomorphological domains, most prominently the Tramuntana Range (1,100 km<sup>2</sup>) in the northwestern part of the island (Fig. 1). The steep topography of this chain, which is linked to its geological complexity and Mediterranean climate, determines intense slope dynamics (Mateos, 2002; Mateos and Azañón, 2005). Practically all the slope movements recorded on Majorca have taken place in the Tramuntana Range. The variety of lithologies cropping out in this mountain chain determines a wide range of slope movements. Landslides and earth flows are frequent phenomena, primarily affecting soft sediments from the Late Triassic (Keuper), made up of clays with gypsum, as well as an entire series of loamy materials from the Palaeogene and Neogene that occasionally outcrop along the mountain range. The historical compilation of the slope movements on the island (Mateos 2002, 2006), as well as the record of those that have occurred more recently, reveal that all processes have taken place after short intense and/or continuous rainfall. During the hydrological years 2008 to 2010, Majorca experienced one of the coldest and wettest winters in living memory. Not only did the accumulated rainfall show twice the average recorded values, this period also witnessed the highest rates of intense rainfall (up to 296 mm/24 h) since instrumental records have been available (1944). These rainy episodes have also coincided with cold periods in which several days elapsed with temperatures around 0° C and as low as -6.8 °C, which are anomalous values in the mild Mediterranean climate. The result was that 34 mass movements were triggered, distributed along the Tramuntana Range, namely 14 rockfalls, one rock avalanche, 15 earth slides- earth flows and 4 karstic collapses. Fortunately, there were no deaths but there were numerous cases of damage to dwellings, holiday apartment blocks, barns and power stations, and especially the road network in the range, most significantly the numerous blockages on the Ma-10 road, which caused significant economic losses in the different tourist resorts.

#### 3.5.2. *Application of the procedure*

Tramuntana range has been monitored using ERS-1/2 and ENVISAT data stacks in descending orbit. The Figure 12 shows a long time series obtained by joining deformation data from ERS-1/2 and ENVISAT results. The final time series covers the timeframe from 1992 to 2009.

### Tramuntana ERS-ENVISAT Displacement time series

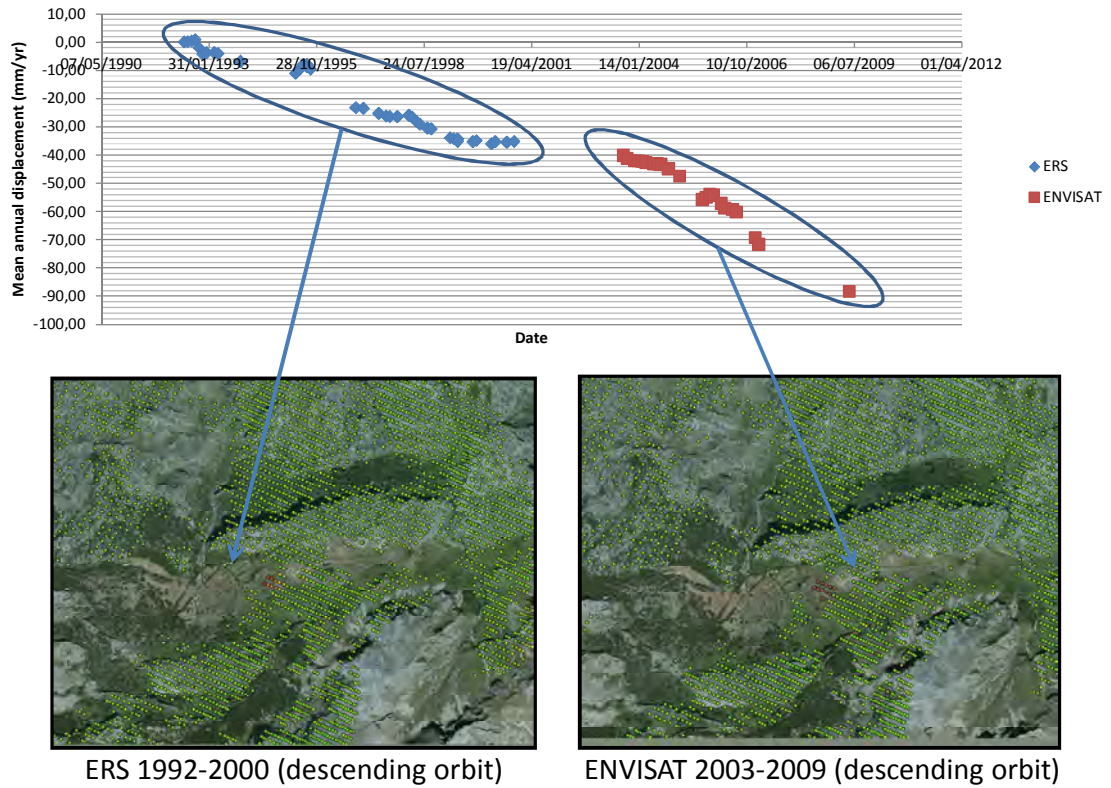


Figure 12. ERS-ENVISAT (descending orbit) displacement time series.

### 3.6. St. Moritz (Switzerland)

#### 3.6.1. *Considered phenomena*

The St. Moritz - Engadine valley area is close to the Piz Bernina in central Alps. In the area Middle and Upper Triassic platform carbonates, mainly dolomites, crop out, overlain by hemipelagic limestone-marl-alternations of Early Jurassic to Early Cretaceous age. The Mesozoic sediments are partly still in contact with the basement, but have also been partly sheared off. Landslides, rock falls and permafrost activities are widespread. Due to climate change, these hazards should be integrated into an inventory and hazard assessment. Satellite and terrestrial SAR interferometry would be an important value added information.

#### 3.6.2. *Application of the procedure*

ERS and ENVISAT IPTA processing was applied in the St. Moritz test area using SAR data of ascending (26 ERS scenes between 1992.05.16 and 2000.10.10 respectively 36 ENVISAT scenes between 2002.10.15 and 2010.09.28) and descending (41 ERS scenes between 1992.06.04 and 2000.10.29 respectively 35 ENVISAT scenes between 2004.05.16 and 2010.10.17) orbits. Only summer images acquired between May and October were considered because of the presence of snow-cover. As a first step, all ERS and ENVISAT SLCs were co-registered to the same ERS reference SLC of the corresponding orbit geometry.

Separate IPTA processing were then applied for the ERS and ENVISAT data stacks, using as reference the scenes of 1999.08.17 for the ERS ascending data, 2006.10.24 for the ENVISAT ascending data, 1997.10.05 for the ERS descending data, and 2007.08.19 for the ENVISAT descending data.

Results for the four processing sequences are shown in Figures 13 to 16 as the average displacement rate. The area of major interest is located in the north of the city of St. Moritz. The SAR images of the ascending orbit show a slight increase of the rate of movement from the ERS (~6 mm/year) to the ENVISAT (~10 mm/year) period. The corresponding time series are however quite linear and do not further disclose any other seasonal or multi-annual change of activity (Figures 17 and 18). The line-of-sight displacement rates of both ERS and ENVISAT SAR data of the descending orbit are on the order of +2 to +3 mm/year. Here, the most interesting feature to observe is the effect of the special SAR imaging geometry, leading to displacements toward the satellite.

The moving area within St. Moritz corresponds to the foot of a large landslide coming down from a few hundred meters above, as nicely shown in one ALOS PALSAR and one Cosmo SkyMed interferogram (Figures 19 and 20). The exploitation of multi-frequency InSAR products will be the subject of Deliverable 3.3.

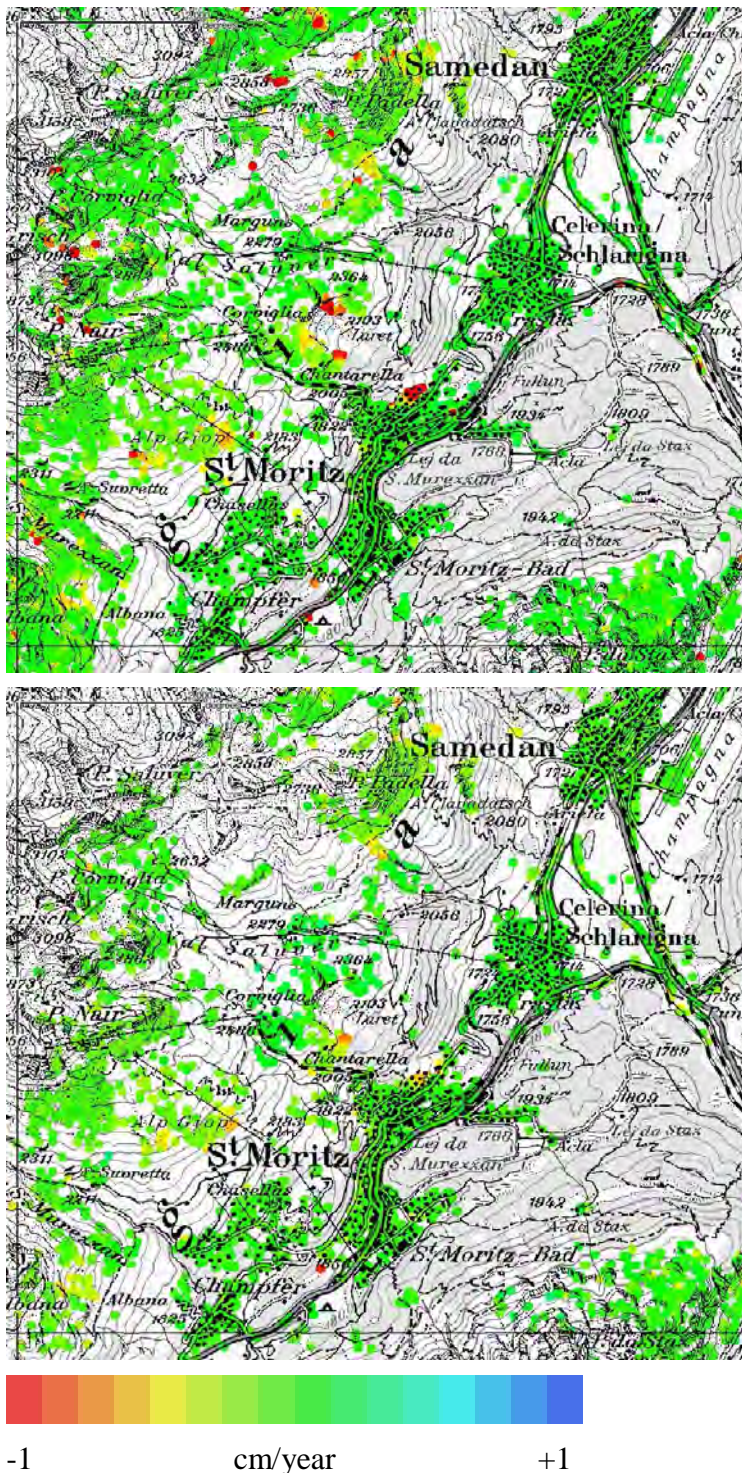


Figure 13 and 14. Line-of-sight deformation rates from ERS (above) and ENVISAT (below) IPTA processing of SAR data of the ascending orbit for the test-area St. Moritz.

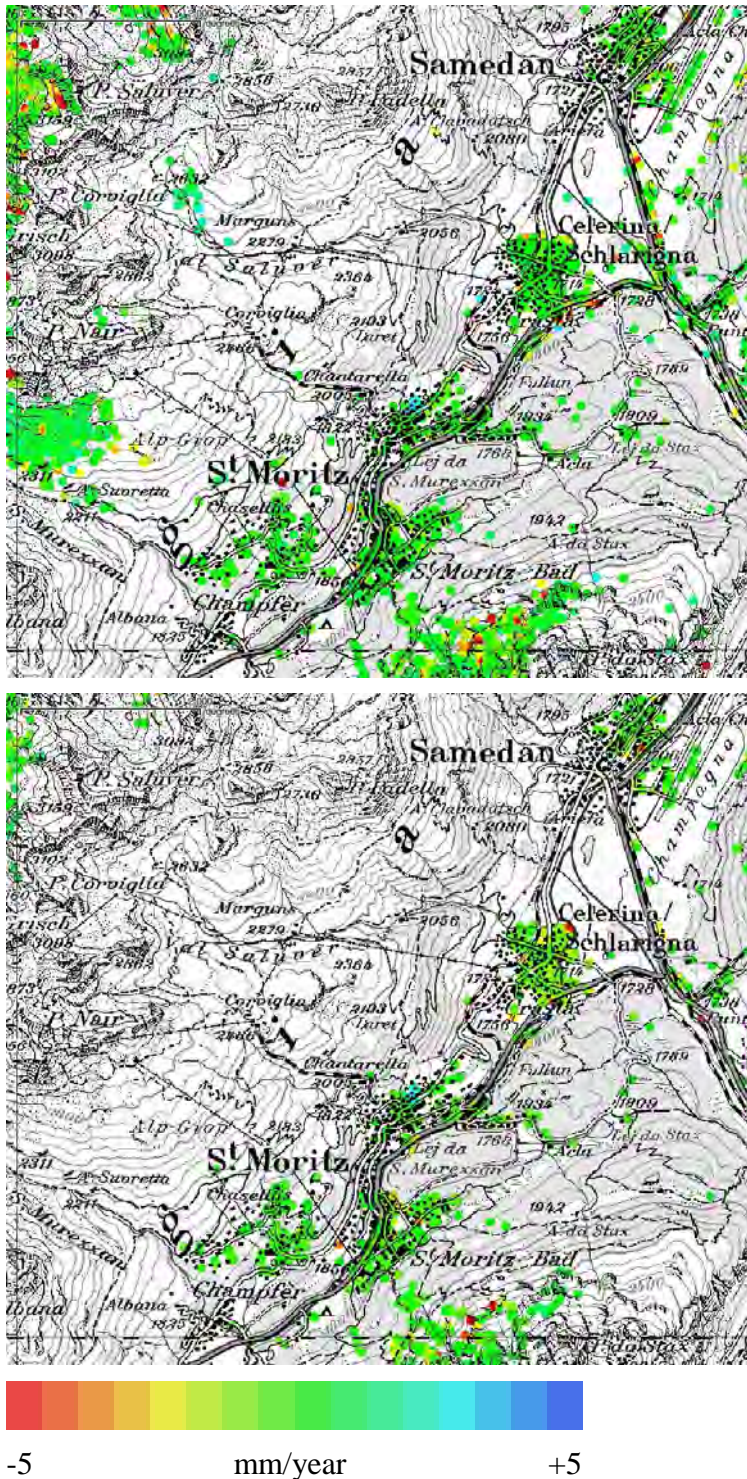
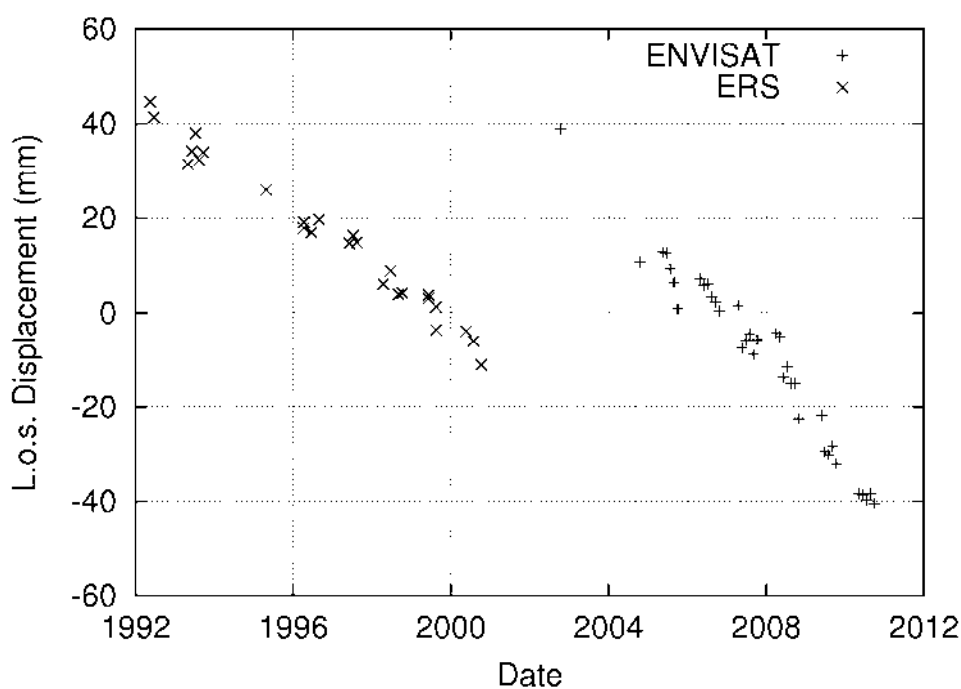
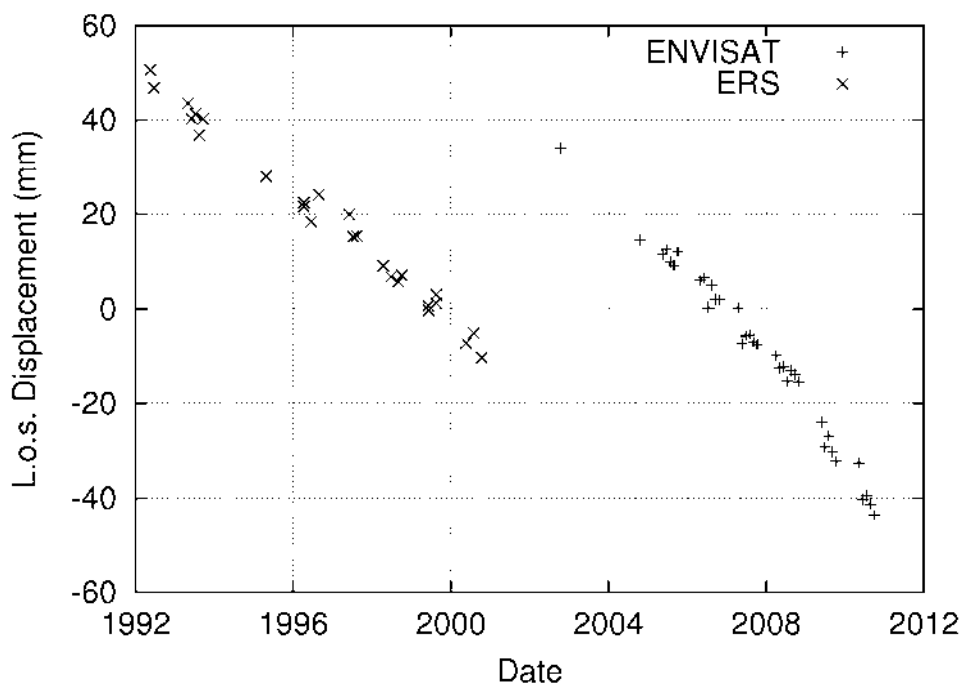
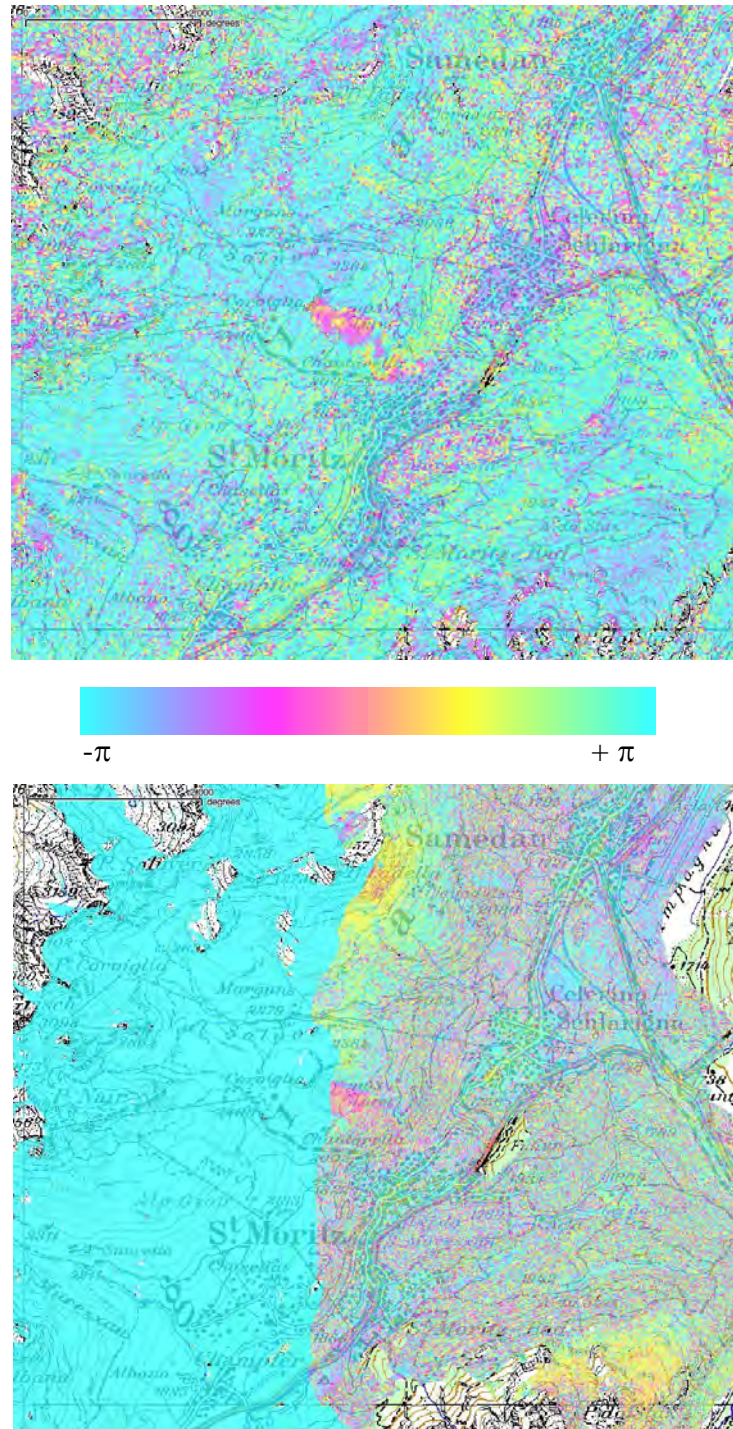


Figure 15 and 16. Line-of-sight deformation rates from ERS (above) and ENVISAT (below) IPTA processing of SAR data of the descending orbit for the test-area St. Moritz.





Figures 17 and 18. Displacement history for two point targets within the moving area to the north of St. Moritz. Above: point coordinates are 784454 E and 152777 N, deformation rates are  $-6.7$  mm/year for ERS and  $-9.7$  mm/year for ENVISAT. Below: point coordinates are 784437 E and 152781 N, deformation rates are  $-5.8$  mm/year for ERS and  $-9.6$  mm/year for ENVISAT. Movements are in the satellite line-of-sight direction, negative values indicate settlement.



Figures 19 and 20 Differential interferograms from ALOS PALSAR data of 20090629\_20090929 (above) and Cosmo SkyMed data of 20110913\_20110929 (below) of the ascending orbit.

### 3.7. Zermatt (Switzerland)

#### 3.7.1. *Considered phenomena*

In the Mattervalley, going up from Visp in the bottom of the Rhonevalley to Zermatt, mainly metamorphic rocks (schists and gniesses) crop out. In the valley there are numerous unstable slopes, including some densely populated regions prone to landslides. Many landslides, rockslides, and rock falls are still active and there are high annually costs for the mitigation and countermeasures. Several large landslides are monitored in the study area, allowing an integration of the InSAR technique for hazard assessment. Numerous active rock glaciers (related to the presence of permafrost in the area) common above 2200 to 2500 m a.s.l., are recognized in the Mattervalley, showing an increasing velocity since the 1980s, in response to a significant permafrost warming. Most active rockglaciers are well detectable with ERS, ENVISAT, JERS, ALOS and TerraSAR-X interferometry at monthly time lapse, whereas the slowest are only visible at yearly interval.

#### 3.7.2. *Application of the procedure*

ERS and ENVISAT IPTA processing was applied in the Zermatt test area using SAR data of ascending (30 ERS scenes between 1992.09.05 and 2000.07.19 respectively 26 ENVISAT scenes between 2002.10.06 and 2010.09.15) and descending (31 ERS scenes between 1995.07.25 and 1999.10.13 respectively 29 ENVISAT scenes between 2002.11.06 and 2010.10.20) orbits (Fig. 21). Only summer images acquired between May and October were considered because of the presence of snow-cover. As a first step, all ERS and ENVISAT SLCs were co-registered to the same ERS reference SLC of the corresponding orbit geometry.

Separate IPTA processing sequences were (Fig. 22) then applied for the ERS and ENVISAT data stacks, using as reference the scenes of 1997.07.30 for the ERS ascending data, 2007.06.13 for the ENVISAT ascending data, 1997.07.30 for the ERS descending data, and 2007.08.22 for the ENVISAT descending data. Because in the Mattervalley displacement rates in the range from several cm's to m's per year are largely present, time series of ERS-ENVISAT displacement rates, highlighting movements in the order of mm's to a few cm's per year, are of marginal interest. Below the ERS and ENVISAT deformation velocity maps from the descending orbit are reported. They indicate many areas moving up to a few cm's per year, but also have large sections without information where movement rates are larger than a few cm's per year.

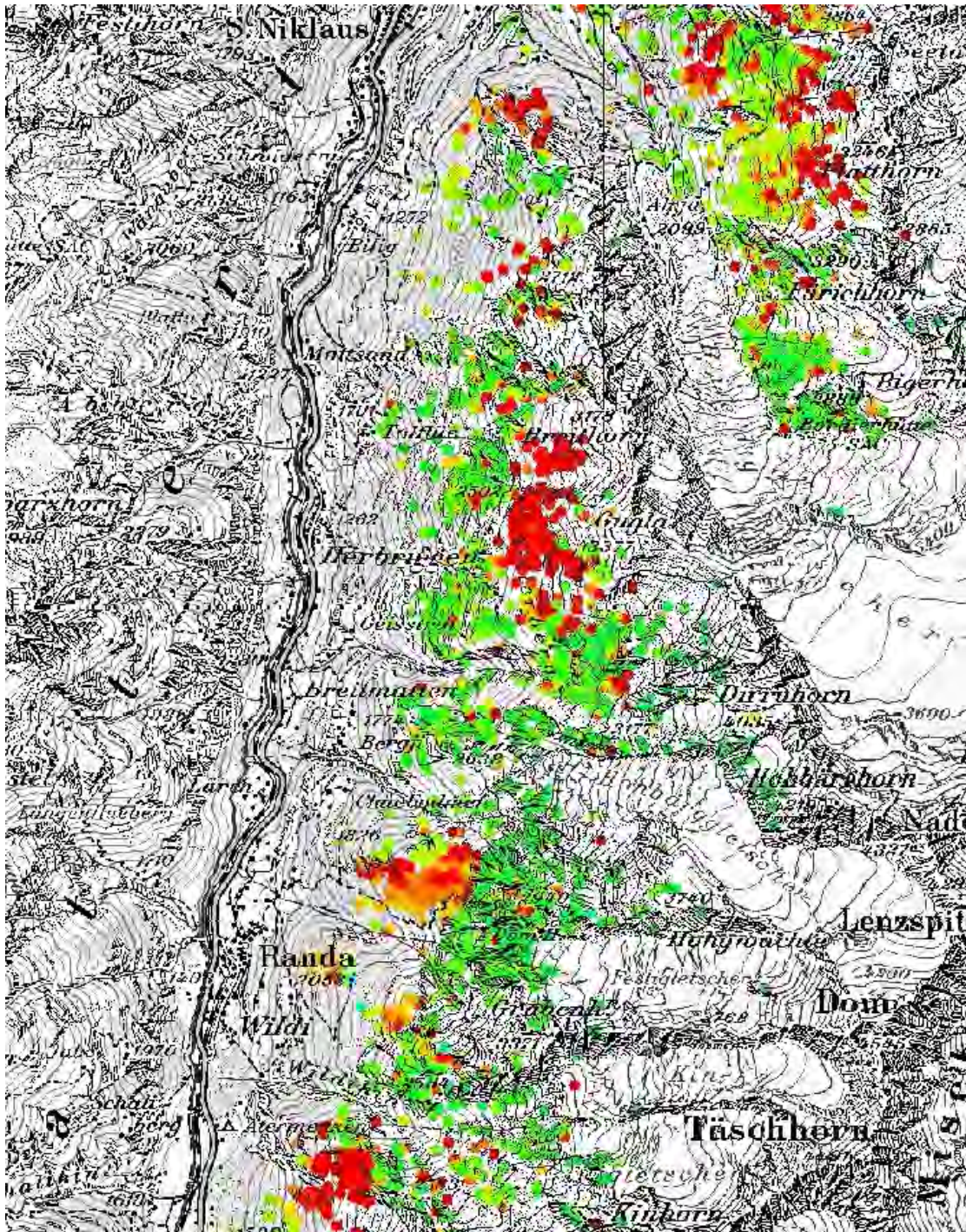


Figure 21. Line-of-sight deformation rates from ERS and ENVISAT data of the descending orbit for the test-area Zermatt.

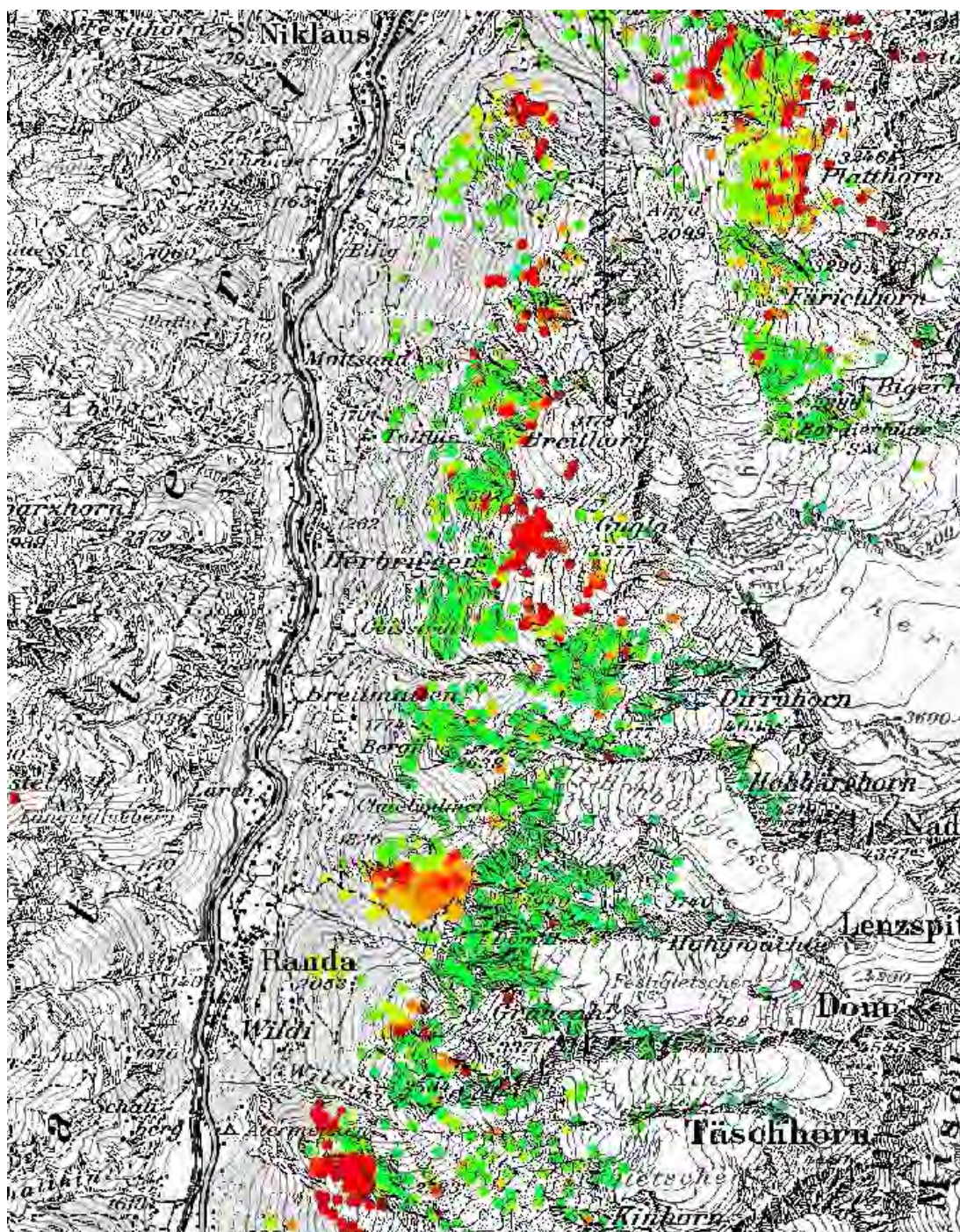


Figure 22. Line-of-sight deformation rates from IPTA processing of SAR data for the test-area Zermatt.

## 4. DISCUSSION

In this section advantages and disadvantages of each developed methodologies will be exploited in order to highlight usefulness of the adopted procedures.

### 4.1. Advantages

Since no model or a priori information is applied, the SBAS approach is particularly suitable for detecting and monitoring non linear deformation phenomena. Thanks to the exploitation of small baseline interferograms, the SBAS approach provides to maximize the number of detected coherent pixels. The integration of ERS and ENVISAT archives allows generating very long term deformation time-series (nearly 20 years) for studying slow-moving phenomena and producing deformation time-series also for areas where the scenes collected by one of the two sensors are not enough for a single-sensor analysis (typically less than 20). The exploitation of ERS-2 post-2000 data allows generating deformation time-series characterized by high temporal sampling. High accuracy in the geolocalization of the coherent targets is guaranteed by the large doppler centroid variability of the ERS-2 post-2000 acquisitions.

The T.R.E. technique uses an extensive archive of satellite radar data (dating back to 1992) to identify networks of persistently scattering features such as buildings and bridges, or natural features such as rocky outcrops, against which relatively-precise motion measurements are calculated retrospectively over the time spanned by the data archive. The main benefit of PSI is its ability to provide multi-year motion histories for individual scatterer points with millimetric precision.

The SPN technique by Altamira uses a stack of SAR images (12-25) to measure ground deformations with very high (millimetric) precision, identifying several ground scatterers not affected by temporal decorrelation, characterized by a reduced level of noise. This technique points to reduce the effect of the atmospheric effects to derive highly accurate elevation and displacement values for each stable point allowing the generation of time series charts very useful for the evolution of the displacement of each stable point. Urban, semi-urban or rural areas can be studied in great detail, both in terms of high spatial resolution and the historical variation of the displacement over long time periods from 1992 up to now.

### 4.2. Disadvantages

Considering the SBAS analysis, the analyzed long time period can produce temporal decorrelation effects, thus limiting the number of targets for which the phase information is preserved for the whole time period; in urban areas this loss of coherent points has been demonstrated to be of about 10%, with respect to the ERS-1/2 1992-2000 analysis. Moreover, in the case of temporally fast varying deformation signals

(i.e., step-like displacements), a short-term analysis (of about 5 years) guarantees better performances of the phase unwrapping procedure, that allow reaching, in these cases, more accurate deformation time-series.

The main limitation of the classic PSI techniques comes from the lack of data in the time period immediately after ERS 2 gyroscope failure. This gap, where no information on target motion can be obtained, exposes to the risk of phase unwrapping errors in the time series (Fig. 23).

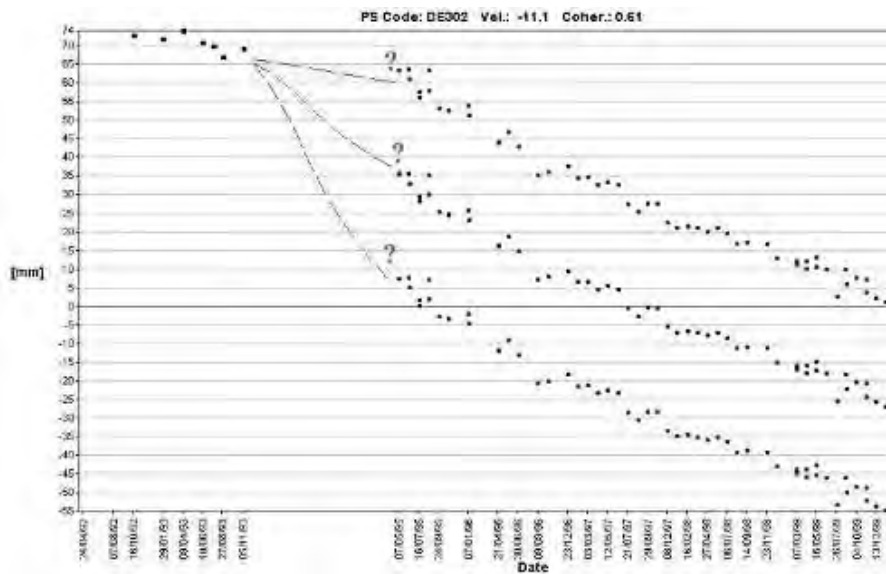


Figure23. Example of phase unwrapping errors in time series.

## REFERENCES:

Berardino, P., Fornaro, G., Lanari, R. & Sansosti, E. 2002. A new algorithm for surface deformation monitoring based on Small Baseline Differential SAR interferograms. *IEEE Transactions on Geoscience and Remote Sensing* 40 (11): 2375-2383.

Bonano, M., Manunta, M., Marsella, M. & Lanari, R. 2012. Long Term ERS/ENVISAT Deformation Time-Series Generation at Full Spatial Resolution via the Extended SBAS Technique. *International Journal of Remote Sensing*, 33, 15, pp. 4756-4783, doi: 10.1080/01431161.2011.638340.

Guzzetti, F., Manunta, M., Ardizzone, F., Pepe, A., Cardinali, M., Zeni, G., Reichenbach, P. & Lanari R. 2009. Analysis of ground deformation detected using the SBAS-DInSAR technique in Umbria, central Italy. *Pure and Applied Geophysics* 166: 1425-1459.

Lanari, R., Mora, O., Manunta, M., Mallorqui, J., Berardino, P. & Sansosti, E. 2004. A small baseline approach for investigating deformations on full resolution differential SAR interferograms. *IEEE Transactions on Geoscience and Remote Sensing* 42: 1377-1386.

Pepe, A., Sansosti, E., Berardino, P., & Lanari, R., 2005. On the generation of ERS/ENVISAT DInSAR time-series via the SBAS technique. *IEEE Geosci. Remote Sens. Lett.*, 2 (3): 265–269.

Wegmüller U., C. Werner, T. Strozzi, and A. Wiesmann, “Multi-temporal interferometric point target analysis”, in Analysis of Multi-temporal remote sensing images, Smits and Bruzzone (ed.), Series in Remote Sensing, Vol. 3, World Scientific (ISBN 981-238-915-61), pp. 136-144, 2004.

Wegmüller, U., C. Werner, T. Strozzi, and A. Wiesmann, ERS – ASAR integration in the interferometric point target analysis, Proceedings of FRINGE 2005 Workshop, ESA ESRIN, Frascati, Italy, 28. Nov. – 2. Dec. 2005.